2-14-2008

Cadherin-Based Adhesion Molecules for Classification of Melanoma with Aqua Technology

Gretchen Melaine Graff
Yale University

CADHERIN-BASED ADHESION MOLECULES FOR CLASSIFICATION OF MELANOMA WITH AQUA TECHNOLOGY

A Thesis Submitted to the

Yale University School of Medicine

in Partial Fulfillment of the Requirements for the

Degree of Doctor of Medicine

by

Gretchen Melaine Graff

2007

Abstract

Cadherin and catenin-family proteins regulate adhesion in malignant melanoma. Using AQUA (Automated Quantitative Analysis) to quantitate the levels of alpha-catenin, beta-catenin, p120-catenin, N-cadherin, E-cadherin, and P-cadherin in melanoma on tissue microarrays (TMA's), we classified 513 patients by protein expression using hierarchical clustering and regression analysis. The dendrogram supported positive correlations seen upon Spearman rho analysis of P-cadherin and beta-catenin ($r=0.5238$, $p<0.0001$) and negative, weak association of N-cadherin with other markers. Patients with high expression of N-cadherin had the highest 20-year survival rate ($p=0.0003$). Our adherens protein molecular classification of melanoma defines at least two distinctive sub-populations of melanoma patients, those with high expression of N-cadherin and those with low expression who have decreased survival. These findings extend previous cDNA array-based findings of an epithelioid class and neural crest class of melanomas.

Acknowledgements

First, thank you to the Yale University School of Medicine Research Department, especially Dr. Forrest, Donna Corranzo and Janet Wooten for providing funding and other support during my first summer of research. The entire department was a great resource for my myriad of questions and concerns. I refined my laboratory technique and grew confidence during my expedition to Bar Harbor for the Intensive Pedagogical Experience. Thank you for this opportunity.

I would like to thank David L. Rimm, M.D., Ph.D. for believing in me and taking me under his wing. His work with quantitative tissue microarrays appealed to my interest in melanoma. He helped me create a project that coincides with my long-term academic and professional aspirations, as well as makes a larger impact on society by increasing our understanding of a very serious disease.

Aaron Berger, an M.D./Ph.D. student, is the source of most of my initial knowledge in this area of medicine. He is an excellent teacher who shared his ideas and dedication with me during my first summer of research. I owe him the credit of such a brilliant project and allowing me to carve my own work from his well-researched, monumental project.

The graduate students who worked in the Rimm laboratory from 2004-2006 were also a source of knowledge and support. I would like to thank Aaron Berger, Derek Pappas, Ph.D., Marisa Dolled-Filhart, Ph.D., Jena Giltnane, and Sharon Pozner. The laboratory technicians who helped me immensely during my time doing research include: Melissa Cregger, Summar Siddiqui, and Kyle DiVito. I would like to thank Malini Harigopal, M.D. for her support and friendly smile each day in the pathology laboratory.

Lori Charette and Joanna Graham from the Tissue Microarray Facility were indispensable due to their work constructing YTMA59 and numerous slides for staining. They were incredibly responsive and very fun people to know.

Thank you to Annette Molinaro, Ph.D. for much needed help understanding some of the statistical analysis. Robert Camp, M.D., Ph.D., Melissa Cregger, and David Rimm, M.D., Ph.D. also provided crucial teaching during my time crunching the numbers.

Finally, my fiancé, Grant Kreizenbeck deserves much credit for providing emotional and moral support for the last 4 years. He has been a sturdy rock in my life. He is always finding ways to make my life easier and better, and I owe much of my success and happiness to him.

Table of Contents

Introduction

Melanoma is predicted to take the lives of approximately 7,910 patients in the United States in 2006, according to the American Cancer Society's age-adjusted statistics. 62,190 people will be diagnosed with the deadly malignancy, 49,710 of those will have melanoma in situ. According to the National Cancer Institute Surveillance, Epidemiology and End Results (SEER) the incidence rate is increasing by 2.8% each year (1981-2002), which is fortunately on the decline from a previously increasing rate of 6.1% (1981-2002) (1). The lifetime risk of developing melanoma for men is now predicted to be 1 in 52 — and for women 1 in 77 (2).

Although melanoma can be a very serious cancer, the survival rates have been increasing in recent years. The relative 5-year survival rate for all races between 1995-2001 was 92%, increased from 85% between 1983-1985, and 80% between 1974-1976(1,2). The death rates in white women have been decreasing since 1988, and for men they have been on a decline since 1998. Although trends from the recent past are showing encouraging new developments, melanoma is still the fifth most common cancer in incidence for men and the sixth most common for woman in the United States (2). Melanoma is the third leading cancer in Incidence Percent Change from 1992-2002 at over 20% risk and over 40% burden for all ages (1).

Melanoma Staging Systems

Statistics show that melanoma proves itself as a deadly malignancy. To determine treatment and prognosis, staging systems provide some ammunition in this difficult fight. Physicians depend on these algorithms to determine how, when, and where (locally or systemically) to treat. Besides guiding treatment, the evidence-based

systems are necessary to estimate survival. Physicians have made great strides to create an accurate melanoma staging system, but the current standards have fallen short of our expectations. When diagnosing malignant melanoma, physicians are forced to provide wide-ranging survival estimates. Balch *et al.* showed that 10-year survival estimates in stage II melanoma range from 50.8% ± 1.7 to 64.4% ± 2.2 and that stage III cancers range from 18.4% ± 2.5 to 63.0% ± 4.4(3). Although predictive of survival, these broad survival estimates are the basis for the most recent American Joint Commission of Cancer (AJCC) staging system. The most recent changes were adopted in 2002, and the current guidelines are based on tumor thickness, nodal involvement, and distant metastasis. The requirements are shown below:

Table 1. TNM Classification of Melanoma (adapted from Kim *et al.* (4)*)*.

Tumor (T) Classification	**Thickness (Breslow)**	**Presence of Ulceration**
T1	< or = 1.0 mm	a: without ulceration b: with ulceration or Clark level IV or V
T2	1.01-2.0 mm	a: without ulceration b: with ulceration
T3	2.0-4.0 mm	a: without ulceration b: with ulceration
T4	>4.0 mm	a: without ulceration b: with ulceration
Node (N) Classification	**Number of involved lymph nodes**	**Level of lymph node involvement**
N1	1 lymph node	a: micrometastasis b: macrometastasis

N2	2-3 lymph nodes	a: micrometastasis b: macrometastasis
N3	>4 metastatic lymph nodes, matted LN, or in-transit met(s)/satellite(s) and metastatic lymph nodes	a: micrometastasis b: macrometastasis c: in-transit met(s)/satellite(s) without metastatic lymph nodes
Metastasis (M) Classification	**Site of Metastasis**	**Serum LDH Level**
M1	Distant skin, subcutaneous, or lymph node metastases	Normal LDH
M2	Lung metastases	Normal LDH
M3	All other visceral or distant metastases	Normal LDH or elevated LDH

Table 2. AJCC Melanoma Stage Groupings (adapted from Kim *et al.* (4)*).*

Stage	T	N	M
0	Tis (in situ)	N0	M0
IA	T1a	N0	M0
IB	T1b T2a	N0	M0
IIA	T2b T3a	N0 N0	M0 M0
IIB	T3b T4a	N0 N0	M0 M0
IIC	T4b	N0	M0
IIIA-C	Any T	N1 or N2 or N3	M0
IV	Any T	Any N	Any M1

Sentinel Lymph Node Biopsy

Since melanoma staging depends on the number of involved lymph nodes, a sentinel lymph node biopsy (SLNB) is a core requirement for complete diagnosis if the tumor depth is greater than 1 mm. Messina et al. showed that immunohistochemistry staining for S100 in the lymph nodes identified an additional 36% of detected metastatic disease than just hematoxylin and eosin stain alone (5).

In 2006, Morton *et al.* tried to further strengthen the argument that the sentinel lymph node biopsy improves survival. They showed that in 1269 patients the disease-free survival rate was 78.3% for the SLNB group and only 73.1% for the observation group (6). Although these numbers are significantly different, it is difficult to argue that an increase survival of 5% is a monumental achievement. The study's melanoma specific death rate was nearly the same for both groups at 5 years (12.5% for SLNB patients and 13.8% for observation patients) suggesting that the effect of the SLNB may not be as powerful as originally believed. Their results confirm that SLNB's are useful to accurately stage melanoma. However, the authors state that early SLNB can also improve disease-free survival (6). This appears true based on their results, but when all the results are carefully weighed, the slight improved survival is not reflected in the melanoma death rate. For their hypothesis that SLNB improves survival to hold true, the effects should be seen across all statistical methods of assessing improved survival.

Lymph node tissue has been the primary material/target for molecular classification of melanoma to date. Researchers stain tissue for S-100 and HMB45, and perform PCR analysis (7). The problem with new models of classification is the process of obtaining lymph node tissue—a SLNB is required. Since melanoma is a deadly

disease, physicians are willing to offer the best possible treatment even if it requires exposing the patient to new risks such as further surgical complications. Sentinel lymph node biopsy is recommended for tumors >1.0 mm, but has had questionable merit in the management of melanoma for tumors <1.0 mm. Ranieri suggests that melanomas >0.75 mm have a metastatic rate of 6.5%, and select patients with other risk factors such as high mitotic activity should undergo SLNB (8). The procedure remains one of the crucial components of our current American Joint Committee of Cancer (AJCC) melanoma staging system (Tables 1 and 2) (9). Any nodal involvement elevates the cancer to stage III. Prognosis estimates using the current system give wide-ranging survival estimates. For example, patients with stage III cancers have survival rates ranging from 18.4% ± 2.5 to 63.0% ± 4.4 (3). These wide ranging estimates are not acceptable. Although few effective adjuvant melanoma therapies exist, we should set out to find further methods to refine the staging of melanoma.

One possible method for determining better survival estimates is the use of molecular classification on primary and metastatic tissue. If clinicians are able to molecularly classify primary tissue into different levels of disease, we could forgo the need for invasive SLNB's.

Molecular Classification of Melanoma

Advances in quantification technologies and analysis algorithms have allowed molecular classification of melanoma on a number of small cohorts. By measuring mRNA expression, Bittner *et al.* separated a cohort of melanoma patients into groups characterized by motility and invasiveness. Although the model was not designed to

relate findings to prognosis, they found that identifying homogenous subpopulations of melanoma patients might allow for better prognosis estimates or possibly more precise treatment for subtypes of melanoma (10). Since these findings, two classes of uveal melanoma have been defined based on gene expression: a "neural crest/melanocyte" class and a more aggressive "epithelial" class. The epithelial class is noted to have membranous staining of E-cadherin and beta-catenin and poor prognosis estimates (11). Other studies have shown that an assortment of genes have variable expression on DNA microarrays when comparing the changes that might occur as a melanocyte changes into a malignant melanoma. The genetic transformations altered protein translation, which was confirmed by measuring protein expression. They investigated genes and proteins involved in: the NOTCH pathway, regulation of transcription, immune modulation, membrane-trafficking, growth suppression as well as many other cellular processes (12). In another study using comparative genomic hybridization, Bastian *et al.* classified thirty cases of melanoma. They used fluorescence *in situ* hybridization to determine that genomic amplification occurs well-outside the histologically demarcated tumor area in acral melanomas. They demonstrated that genomic changes seen in invasive melanoma are present in earlier stages of melanoma progression, by showing the same molecular aberrations in melanoma in situ (13). Therefore, by classifying tumors molecularly, sub-types of melanoma can be distinguished even in the very beginning stages of carcinogenesis.

Alonso and colleagues have completed the most significant study of this type using tissue microarrays to molecularly classify melanoma. The examined expression of thirty-nine markers on 165 cases of melanoma, evaluating cell cycle and apoptosis related

proteins in a qualitative manner. They created a four-marker predictor model that was validated with a different cohort and was found to be predictive independent of Breslow depth of invasion (14). However, they did not use a quantitative form of immunohistochemistry and used only seventy-two melanoma cases to validate their predictor model. Our work will build on these findings by quantitating differences in protein expression to classify a larger cohort of patients into prognostic groups.

Using immunohistochemistry on tissue microarrays to classify melanoma has many advantages such as the ability to work easily with a large number of samples of patient tissue, but the technique is limited by the quality and availability of effective antibodies. During scientific exploration it is important to ask the right question, but even more important than asking the correct question is the attainment and validation of the supplies used to seek the correct answer.

Treatment of Metastatic Melanoma

The standard of care as a primary modality of treatment for malignant melanoma is surgical resection of the tumor with boundaries of 2 mm for those with melanoma of > 4.0 mm in thickness (15,16). Many feel that SLNB is also part of the standard of care to date (15,17). Patients with local recurrence or metastatic disease should receive adjuvant therapy (15).

Most adjuvant therapies for stage IV metastatic melanoma patients are still in investigational stages, and the few forms of therapy that have been used in practice are not ideal. There is no clear treatment of choice because many of the adjuvant therapies only help small percentages of patients in clinical trials; patients typically respond for

only a few months. However, dacarbazine and hydroxyurea are currently the only cytotoxic treatments approved by the FDA to treat metastatic melanoma (18). Hydroxyurea has not been used as commonly as dacarbazine. The former drug's effects on metastatic melanoma have been investigated for over thirty years, and although it is the "standard of therapy" it only shows response rates of 15-25%. In less rigorous studies small percentages of patients had been shown to survive up to 6 years, but these studies are typically not reproducible (18). Various studies using dacarbazine alone or in other regimens show median survival ranging from 4.6 to 11.9 months (19). Although the survival time for patients with metastatic melanoma is only 6 to 9 months, minimal improvement in survival comes at a price since all medications have side effects and typical chemotherapeutics have very toxic side effects. A meta-analysis of recent "level 1" evidence studies have shown that dacarbazine as a single agent is as effective as multiple-drug regimens (19). They point out that few quality of life studies have been completed, but typical side effects of nausea, vomiting, fatigue, neutropenia, thrombocytopenia, and anemia are considerably lower when taking dacarbazine as monotherapy verses in a 4-drug Dartmouth regimen (dacarbazine, cisplatin, carmustine and tamoxifen) (19).

All current forms of cytotoxic therapy typically show low response rates of less than 25%. Researchers have been creative in searching out other treatments beyond typical chemotherapeutics that may show efficacy. Scientists have tried tamoxifen, thalidomide, interferon-alpha, and interleukin-2. The immunomodulators have response rates ranging from 40-60%. Other treatments currently under early investigation in mostly Phase 1 and 2 clinical trials include: sorafenib (a BRAF kinase inhibitor), human

anti-CTLA-4 monoclonal antibodies, anti-BCL2 antisense oligonucleotides, and integrin monoclonal antibodies (MEDI-522) (18).

A very recent Phase II study employing the use of dacarbazine as well as two immunomodulators interleukin-2 and interferon-alpha, has shown one of the best response rates and most promising survival effects to date. They measured the size of metastatic tumors as well as disease-related symptoms to determine an overall response rate of 52%. Median survival for partial responders was 27 months, while the few patients who had a complete response with remission of symptoms and disappearance of metastatic lesions for 4 weeks had an average survival of over 36 months. The median survival of non-responders was 15 months. Although this is a very promising study, the majority of patients had only a single site of metastasis in soft tissue or a lymph node (20).

In conclusion, there is no clearly effective single adjuvant therapy regimen for metastatic melanoma patients. Learning more about the biology and subtypes of melanoma might allow us to develop more precise and effective therapies.

Cadherin and Catenins in Melanoma

Cancer metastasis is a crucial factor in determining patient prognosis. Cells must detach from their surroundings, migrate to the blood stream, then grow and survive in a new environment. Scientists are progressively learning which factors are important for each step. For carcinoma cells to separate from neighboring cells, proteins that allow adherence must be downregulated or destroyed (21). Voura *et al.* showed that during flow through the bloodstream, melanoma cells will interact with endothelial cells via

pseudopods and structures composed of F-actin (22). The final steps of metastasis require the displaced tumor cells to "latch on" to cells in a new environment and then continue to grow and divide. Our research will focus on the first stage of tumor metastasis during which cells detach from their surroundings by altering amounts of specific proteins that make up the adhesion complex.

The adhesion complex is composed of a variety of cadherins and catenins that maintain the cell's integrity with its environment. Cadherins are calcium-mediated, adhesion glycoproteins that allow cell-to-cell interaction (Figure 1). Catenins, cytoplasmic proteins, compose part of the adherens junction and are thought to be a part of the signal that assures contact inhibition. The proteins secure the actin cytoskeleton to the cell membrane. Cadherins and catenins interact to mediate cell adhesion. E-cadherin, as well as P-cadherin or N-cadherin, can bind directly to beta-catenin and p120-catenin. Beta-catenin can then bind non-actin bound alpha-catenin. N-cadherin is typically found in neural cell types, while E-cadherin is associated with epithelial tissue. P-cadherin is typically found in embryonic tissue, but can be present elsewhere. E-cadherins bind to each other via homotypic interactions (23).

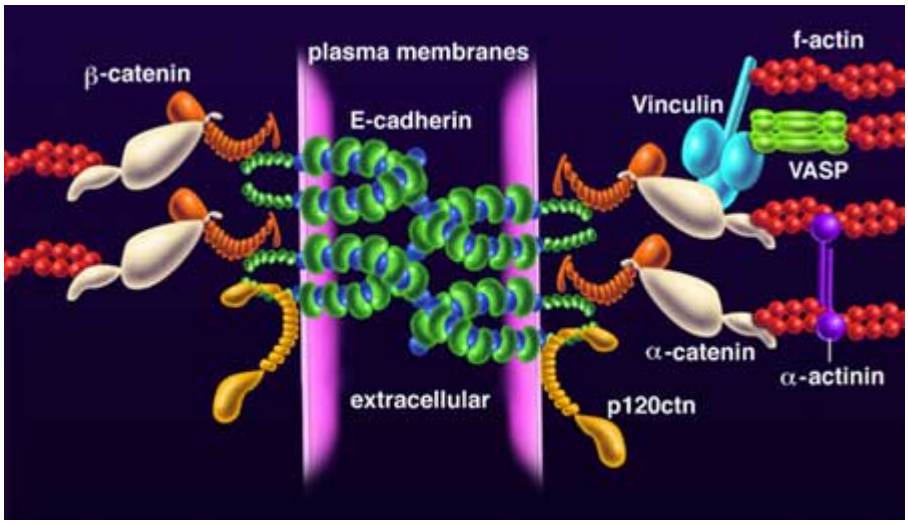

Figure 1. **Cadherin and Catenin Biology.** (© humpath.com adapted from http://www.humpath.com/IMG/jpg/adherens_junctions-2.jpg).

Numerous malignancies including carcinoma of the esophagus, colon, stomach, and breast have shown decreased levels of cadherin and catenin proteins when compared to normal tissue particularly in more aggressive tumors (24-26).

Melanoma follows a similar pattern of loss of adherens junctional proteins when it becomes more invasive. Decreased expression of E-cadherin in malignant melanoma indicates worse disease-free survival for patients (27). Low expression of E- and P-cadherin seem to correlate with disease progression in melanoma (28). Unquantitated immunohistochemical studies show a decrease in P-cadherin from primary to metastatic melanoma, but no significant changes in E- or mesenchymal N-cadherin (29). Similar studies show that maintaining P-cadherin expression is associated with better survival in small tissue microarray cohorts (30). In reconstructed skin models P-cadherin exhibits decreased metastatic invasion with retained expression independent of N-cadherin (31). However, some studies with further refined methods of subcellular localization of marker expression have found that E-cadherin, P-cadherin, and beta-catenin shift between the nucleus, cytoplasm and membrane depending on tumor thickness and patient survival. They used univariate and multivariate analysis to show that membranous N-cadherin staining, cytoplasmic P-cadherin expression and loss of membranous E-cadherin correlated with thicker and more aggressive tumors (32).

The catenins exhibit similar trends. Alpha-catenin expression is reciprocally related to tumor thickness, suggesting that low alpha-catenin would correlate with a poor prognosis (33). A decrease in expression of beta-catenin is seen comparing primary melanoma to metastatic disease (29). A paucity of beta-catenin within carcinogenic

melanocytes is significantly associated with thicker tumors and decreased survival (32). Very few studies have investigated the role that p120-catenin plays in melanoma, but one study shows that p120 expression is correlated to beta-catenin expression in melanoma. Other correlations to tumor thickness and comparisons between primary and metastatic melanoma were not significant (33). Gamma-catenin often has little to no expression in nevi or melanoma samples using immunohistochemistry (29,34). Despite this progress, few studies show prognostic implications for immunohistochemical data and none show quantitated expression of nearly all classic cadherin and catenin markers in a large cohort.

To further molecularly classify malignant melanoma, we investigated the relationships among alpha-catenin, beta-catenin, p120-catenin, N-cadherin, E-cadherin, and P-cadherin in melanoma tissue using quantifiable immunohistochemistry. Patient subpopulations were created using hierarchical clustering based on protein expression patterns, and then further assessed for survival to answer the most important question: "Does molecular classification predict a patient's length of survival?"

Hypothesis

In human melanoma tissue, does the expression pattern of six adhesion complex proteins: α catenin, β catenin, p120-catenin, E-cadherin, N-cadherin, and P-cadherin classify patients into distinctive sub-populations? Does molecular classification predict survival?

Aims of Thesis

Aim 1:

First, we collected clinical information from a cohort of melanoma patients to use in an analysis of protein expression from primary and metastatic melanoma tissue.

Second, we selected appropriate markers that have been previously implicated in the progression of melanoma through a complete literature review. After validating the selected six antibodies, we measured cadherin and catenin expression in primary and metastatic melanoma tissue from the cohort of patients, melanoma cell lines, and nevi. We used immunohistochemistry on tissue micro-arrays with an automated system to analyze protein expression. By staining with anti S-100 antibody concurrently with each marker antibody, we created a tumor mask for each sample to demarcate melanoma in epithelial tissue. DAPI staining was used to distinguish nuclei from cytoplasm. The overall score of protein staining was recorded.

Aim 2:

The relative levels of protein were linked and then analyzed with each patient's prognostic information (using Kaplan-Meier curves, COX analysis, and hierarchical

clustering) to detect whether molecular classification of melanoma could indicate prognosis.

We hypothesize that there is a positive correlation between cadherin or catenin expression and survival. The hope is possibly to relieve the need for a sentinel lymph node biopsy. Technicians could perform immunohistochemical staining to detect the aggressiveness of malignancy, and then determine the likelihood that the melanoma will spread to other areas of the body. Therefore, patients might be spared the painful – and not always predictive – procedure of sentinel lymph node biopsy. Additionally, physicians will be able to better predict the aggressiveness of each specific case of melanoma. As successful treatment modalities are identified, clinicians will be able to more confidently guide patients to patient-specific treatment plans. Hopefully the patients who need adjuvant therapy will be more readily identified.

Methods

Melanoma Tissue Microarrays (TMAs)

In order to systematically classify large cohorts of patients based on molecular expression of proteins, scientists must have an effective and reproducible means of performing these potentially large experiments. One such method employs the use of tissue microarrays to decrease the amount of tissue used in each experiment as well as ease the required work and time demands that traditional slides would demand. Figure 2 illustrates the steps to create a TMA.

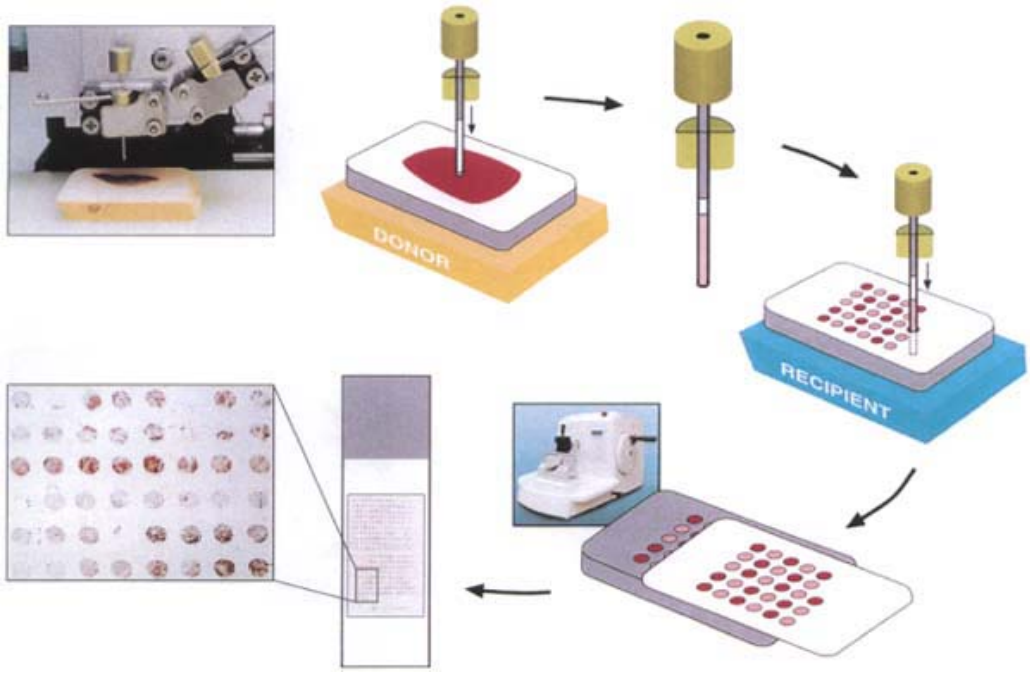

Figure 2 (35)**. Tissue Microarray Construction**. After a pathologist identifies the area of interest, a core of sample tissue is drilled using a precision arraying instrument. The cores are placed in a paraffin recipient block. Using a tape transfer system, 5-micrometer thick sections are sliced from the block and cross-linked to slides. The final image shows an example section of histospots on a slide. Each histospot is assigned a specific grid location used to identify the spot after staining.

Some benefits of working with TMA's include the conservation of human tissue which is of limited and coveted supply, and the reduction of slide-to-slide staining variability that would be seen if comparing traditional slides. A downfall is that only a small section of original tissue is represented on each slide, and a great percentage of the tissue architecture is not represented. However, representative tissue is carefully selected by pathologists when used in a TMA.

For our study, formalin-fixed, paraffin-embedded specimens from the archives of the Yale University Department of Pathology were used to construct YTMA 59. YTMA 59 is a compilation of 512 melanoma specimens with nearly complete follow-up for every case, including cause and date of death. All patients were diagnosed between 1959 and 1994. The array consists of primary (215), metastatic (283), and local recurrence (14) specimens, along with nevi (22) and melanoma cell lines (mm127, mnt1, sk23, mel888, mel624, melanocytes1, yugen8, yumac, yumor, yusac2, yusit1, 1241, 1335, 501, 928) as negative and positive controls, respectively. Descriptive characteristics of the patients and melanoma samples from YTMA59 are summarized in Table 3.

Table 3. Descriptive statistics of patients with melanoma tissue on YTMA59.

	N	Primary Melanoma	Local Recurrence	Metastatic Melanoma
Cohort	511	214	14	283
Age, mean (yrs)	469	57.8	57.6	53.3
Female	225	111	5	109
Male	272	102	9	161
Breslow, mean (mm)	260	2.47	5.20	3.03
Stage I-IIB	264	158	11	95
Stage III-IVA	89	30	1	58

To construct the TMA, we identified representative areas of melanoma, nevi, or cell lines and placed 0.6 mm diameter cores into a recipient block using a precision arraying instrument (Beecher Instruments, Silver Spring, MD). An ultraviolet, cross-linkable, tape transfer system (Instrumedics Inc., Hackensack, NJ) fastened 5-micrometer sections to adhesive slides.

Each master block has each case represented by a single histospot. Every 10th slide is stained with H&E and reviewed by a pathologist to confirm the diagnosis of melanoma. An internal reviewer observed all histospots during staining. The slides were enveloped with paraffin for storage. Each slide was cut as needed, but if storage was required slides were placed in a nitrogen desiccation chamber to prevent antigen oxidation. We have shown that these methods successfully store slides for up to 3 months (36).

Students working in the Rimm Laboratory prior to 2004 collected the patient data for YTMA 59. I assisted with data collection for a new YTMA while working in 2004.

Fluorescent Immunohistochemical Staining

Fluorescent immunohistochemical staining utilizes immunologic interactions between primary and secondary antibodies to link a fluorescent probe to a specific protein target. Coons and colleagues were first to successfully link a fluorescent dye to antibodies using the principles of immunohistochemistry (37). The general principles and steps of immunohistochemistry are as follows: 1) antigen fixation: the tissue is prepared (usually using formalin or paraformaldehyde) to preserve histological architecture and cellular shape; 2) tissue sectioning: typically specimens are embedded in

paraffin wax or a whole mount can be prepared to give 3-dimensional cellular information; 3) antigen retrieval: methods such as pressure-cooking slides in citrate buffer or reagents like proteinase K, trypsin, or pepsin are used to disrupt the protein cross-links from formalin fixation to unveil hidden epitopes; 4) blocking of background staining: hydrogen peroxide will prevent non-immunologic staining; 5) direct or indirect linkage of antibody to antigen and detection source: direct antibodies have a detection source previously bound to the antibody, while indirect methods use a primary antibody to bind to antigen, then a secondary antibody binds to primary antibody because it is against the IgG of the specific animal in which the primary antibody was grown; indirect linkage allows for detection amplification; the secondary antibody is typically conjugated to biotin or horseradish peroxidase, and finally colorimetric agents such as DAB, or linked fluorescent dyes such as cy5-tyramide, are added to allow for detection (38).

With the use of an epiflourescent microscope, we are able to locate molecular targets. The natural tissue architecture is maintained because of *in situ* hybridization, allowing us a more accurate assessment of molecular targets. We chose automated quantitative immunohistochemistry because it even further standardizes the traditional methodology of grading staining. Pathologists typically have relied on manually scoring each slide as "0, 1+, 2+, 3+" in staining intensity. However, this traditional visual assessment of each slide is time-consuming and subject to bias from individual raters. Our laboratory has created a reliable system of automated quantitative immunohistochemistry to forgo the downfalls of traditional manual staining techniques (39).

Each TMA slide was first deparafinized using xylene, followed by one wash in 100% ethanol and then further diluted washes (95%, 90%, etc.) down to 50% ethanol and 50% water for three minutes at each dilution. The slides were transferred to deuterium depleted (dd) water and boiled in a pressure-cooker in 6.5 mM Na-citrate buffer (pH 6.0) for 15 minutes. Endogenous peroxidase activity was blocked using a solution of using absolute methanol with 0.75% hydrogen peroxide for 30 minutes at room temperature. The slides were washed with tris-buffered saline (TBS) twice, and then incubated with 0.3% bovine serum albumin (BSA)/1x TBS to diminish nonspecific background staining. The following primary antibodies were used on separate slides at the following dilutions: mouse anti-α-catenin (Zymed Laboratories, 180225, Clone CAT-7A4) 1:150, mouse anti-β-catenin (BD Transduction Laboratories, 610153, Clone 14) 1:2500, mouse anti-E-cadherin (BD Transduction Laboratories, 610181, Clone 36) 1:400, mouse anti-P-cadherin (BD Transduction Laboratories, 610227, Clone 56) 1:250, mouse anti-N-cadherin (Zymed Laboratories, 18-0224, Clone 3B9) 1:150, mouse anti-p120-catenin (BD Transduction Laboratories, 610133, Clone 98) 1:400. The proper dilution for each primary antibody was determined after staining melanoma test arrays at four different dilutions based on values found in the literature. Envision goat anti-mouse-horseradish peroxidase was used as a secondary antibody. All antibodies used in this study have been previously validated and used by our laboratory (40-42). Subcellular localizations are all consistent with previous descriptions for each antigen. Using 4', 6-diamidino-2-phenylindole (DAPI) staining (1:100) we were able to differentiate each cell's nucleus from cytoplasm. S-100 was used to stain each case and define a region of interest (mask) for the melanoma within each sample histospot at a dilution of 1:650 (DAKO) (43).

Staining for gamma-catenin at various dilutions was attempted, but due to nonspecific staining the additional protein marker was abandoned. Additionally, because melanoma tissue rarely expresses gamma-catenin the possibility exists that staining may have been accurate but not sufficient for our analysis.

I worked with a fellow medical student, Aaron J. Berger, to learn the immunohistochemistry technique. For nearly half of the markers, we worked together on the staining. I also assisted him in staining other potential markers at various concentrations for his dissertation. Besides my own adhesion protein antibodies, I performed the staining and titrations for the following markers while occasionally utilizing Berger's assistance: HIF-1alpha, ki67, p16, p21, p27, p53, cyclin D1, nm23. Laboratory technicians, including Kyle DiVito, Melissa Cregger, Summar Siddiqui,, occasionally mixed solutions for general staining purposes. I created my own dilutions of antibodies.

Quantification

Histospot images were acquired using a modified computer-controlled epifluorescence microscope (Olympus BX51 microscope with automated *x*, *y*, *z* stage movement.) and an Olympus Motorized Reflected Fluorescence System and software (IP lab v3.54, Scanalytics, Inc.), with an attached Cooke Sensicam QE High Performance camera. The customized system automatically obtained images at the specified wavelengths.

Dr. Robert Camp of our laboratory created a custom program that "finds" all histospots and creates a system of identification utilizing the rows and columns. The

"spotfinder" algorithm uses size criteria to initially find all the locations, and then uses the known grid system to identify the other tissue samples. The coordinates of all the histospots are recorded to be used for linkage to clinical data (Figure 3).

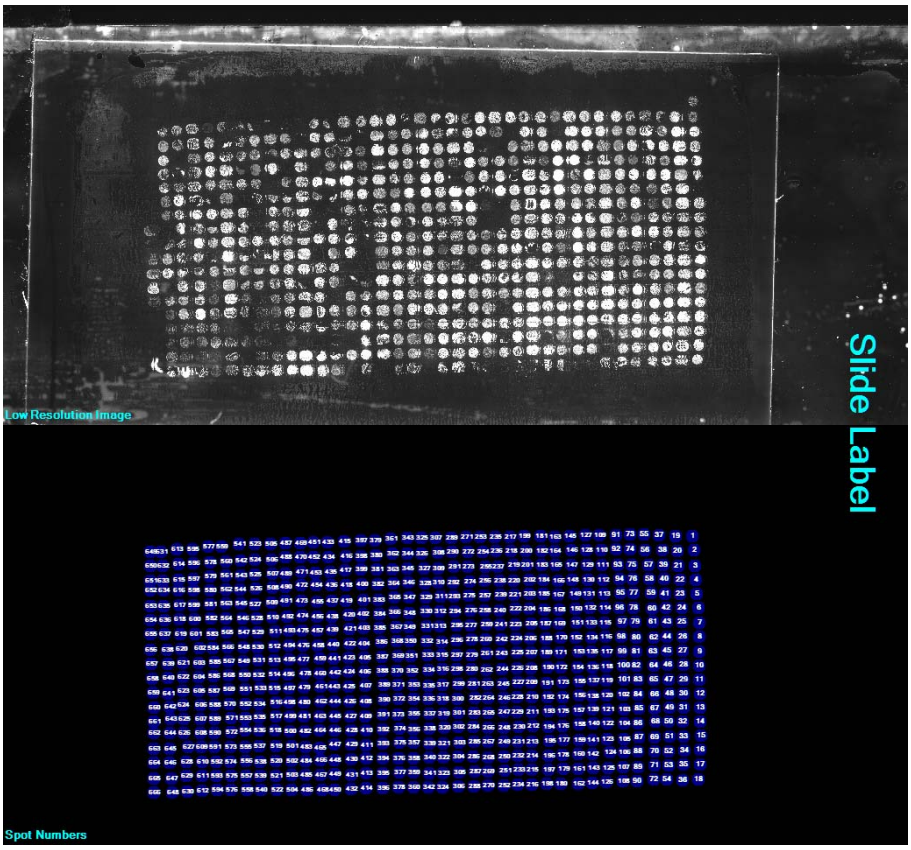

Figure 3. Microarray image after spotfinder algorithm.

Tissue staining was graded on a scale from 0 to 4095 using the program AQUA (Automated Quantitative Analysis), designed by Dr. Robert Camp. It allows for computerized accession and quantification of tissue microarray protein levels. The Rapid Exponential Subtracting Algorithm (RESA) produces a "non-nuclear mask" by subtracting the DAPI (nuclei) image from the larger S100 (tumor mask) image for each histospot. AQUA and RESA have been previously described by Camp et al. (Figure 4) (39).

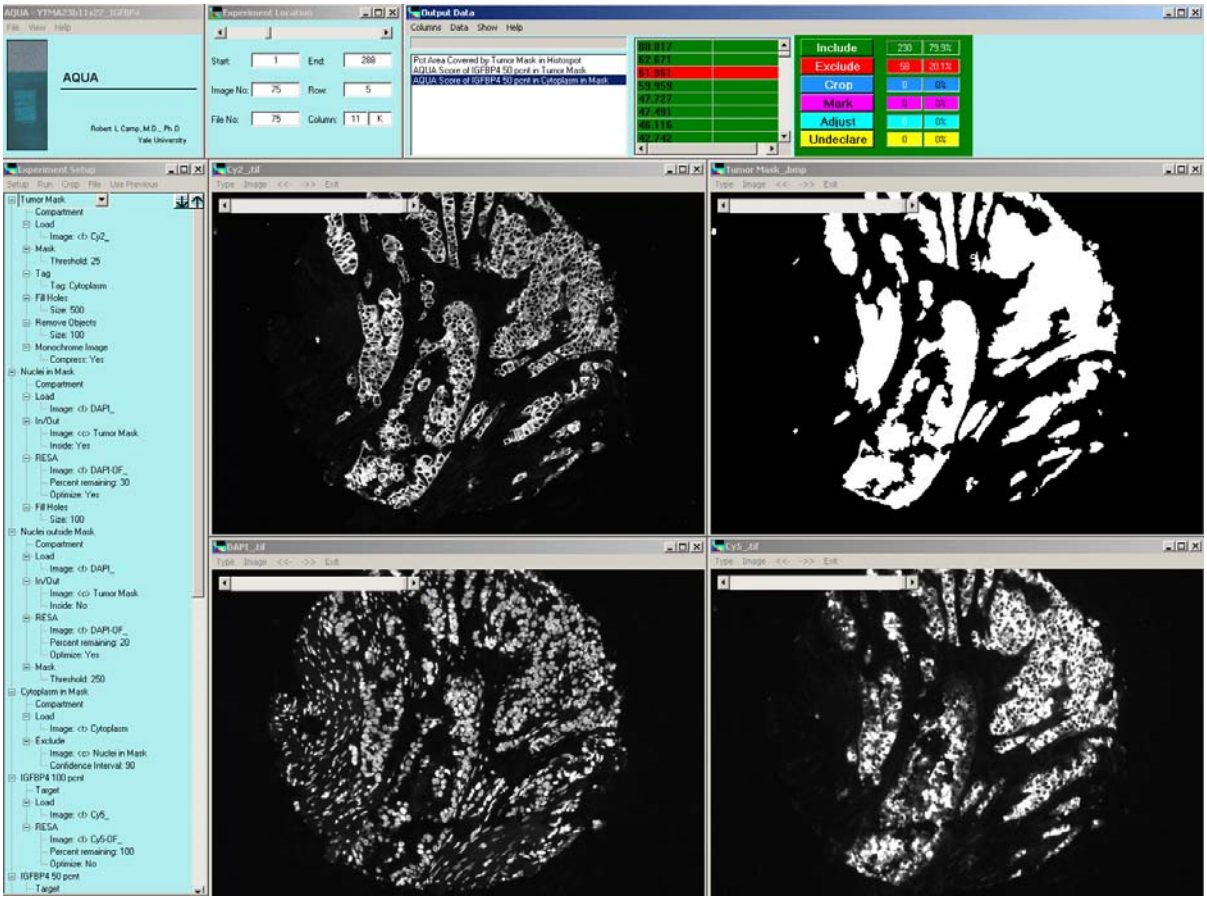

Figure 4 (adapted from Aaron J. Berger 2006). AQUA software. The panels above show the title pane, score window, settings window, algorithm window and four image windows with raw and processed data from one example histospot. The upper left image shows an original keratin immunofluorescence picture before the tumor mask is applied. The upper right image window illustrates the tumor mask. The lower right pane demonstrates the non-nuclear (cytoplasm) mask.

In brief, the computer and microscope system utilize two images, one taken at the appropriate plane of focus and an additional image taken below the previous plane. The second image is essentially just below the base of each 5-micron section of tissue. The two high quality, monochromatic 0.5 micron resolution images allow for the distinction of large subcellular compartments such as nuclei (39).

AQUA uses the following two algorithms, RESA and PLACE (pixel-based locale assignment for compartmentalization of expression), to: 1) create each "tumor mask," or

identify tumor within other tissue; 2) identify large subcellular compartments; and 3) quantify and locate biomarker florescence within tumor mask.

Using co-localization to measure the amount of target within the previously defined "mask," an AQUA score is determined for the entire tumor area, as well as for the nucleic area and "non-nuclear" area (i.e. mostly cytoplasmic area). AQUA scores are continuous variables and defined as (intensity of target)/area (Figure 5).

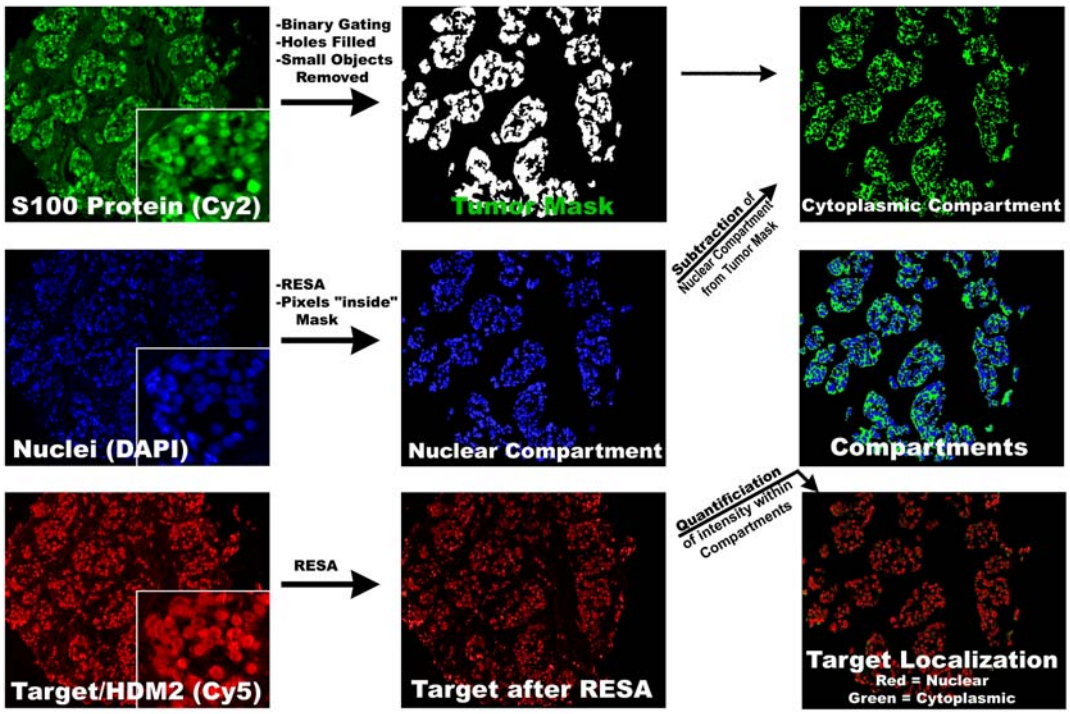

Figure 5 (adapted from Aaron J. Berger 2006). AQUA algorithm for melanoma. The first column of images is raw, while the last column is post-AQUA melanoma protocol. The first row of windows shows S100 protein expression (Alexa 488), a marker specific for melanoma in epithelial tissue. The expression of S100 differentiates tumor from surrounding tissue. The individually produced tumor mask is captured as a binary image, and further refined by removing small objects and filling holes. Next AQUA relies on the DAPI image to discriminate nuclei. Using RESA (Rapid Exponential Subtracting Algorithm), the DAPI (nuclei) image is subtracted from the larger S100 (tumor mask) image to produce a non-nuclear (cytoplasm) mask. The final images in the bottom horizontal row show RESA application to the target (HDM2) image. Cy5 immunofluorescence is used to capture specific marker staining. RESA uses exponential subtraction to obtain the most precise quantification via pixel-based locale assignment for compartmentalization of expression (PLACE algorithm). Following image acquisition, the aforementioned masks are applied. The target localization image in the lower right corner illustrates the final image used to quantitate the AQUA score, which is intensity/area.

Aaron Berger assisted me with the initial marker acquisitions, but after learning the programs I set up and ran AQUA for my markers.

Statistical Analysis

Only histospots with tumor covering greater than 5% of tissue area were included in our analysis. The specimens were linked to their respective prognostic information using Cruella online. We used JMP 5.0.1, Statview 5.0.1 (SAS Institute Inc., Cary, NC), and X-Tile software (http://www.tissuearray.org/rimmlab/xtile.html) for data analysis. Survival curves were created using the Kaplan-Meier method (univariate analysis)(44). The values of cadherin expression in the non-nuclear mask were used whenever these markers could be analyzed separately to allow for more precise data interpretation. The Cox proportional hazards test was used for univariate and multivariate analysis. Non-normally distributed raw data was normalized using the natural log before individual parametric tests. Otherwise, raw AQUA scores were always used during analysis. Significant results required a p value of <0.05.

Non-Parametric Spearman Rho Scatterplot Matrix

A scatterplot matrix shows the magnitude of similarity or dissimilarity among numerous markers. The matrix system allows for the comparison of each individual marker to every other marker by first ranking the data, then calculating the scatterplot matrix. The rho value denotes the degree of similarity, or "linear relationship," and can be positive or negative suggesting the type of association (direct or inverse) (45,46).

X-Tile Software

To create the Kaplan-Meier survival curves, we used X-Tile software to find the optimal binary cut-point in our data. We split our cohort into a training and validation set. Each set contained half of our original cohort and was outcome matched. The training set was used to define low- or high-expressing melanoma tissue for each specific marker. We then tested the cut-point on the validation set to assess the prognostic value of each marker (47).

Hierarchical Clustering

For hierarchical clustering, we first applied the natural log to tumor mask AQUA scores to normalize raw data. Z-scores were produced from the normalized data and values were analyzed with Cluster 2.11.0.0 and Gene TreeView 1.60 (http://rana.lbl.gov/EisenSoftware.htm). Using 80% present as the filter, 395 patients out of 514 were included in the tree following average link clustering. Four minor clusters equidistant from the patient cluster were arbitrarily chosen and analyzed with Kaplan-Meier survival curves.

Hierarchical clustering is a way to separate sub-groups of patients by similarity of their expression profile. The idea is to cluster patients who are more similar to each other than everyone else in the cohort by comparing each patient's expression profile with all other patient's profiles. The analysis creates sub-populations by minimizing differences within clusters and maximizing differences between different clusters. The process of clustering produces a dendrogram of patient profiles and biomarkers. The branch length

describes the extent of similarity. Different "clusters" may be chosen to group patients by selecting a point along the length of the patient dendrogram. Any point may be chosen depending on how similar or dissimilar the groups are desired to be. Additionally, the biomarkers also are placed in a dendrogram that suggests similarity or dissimilarity of staining patterns. Patients, with their expression profiles, are placed in order to create a "heat map." The color and intensity (typically red denotes high expression and green shows low expression) describes the quantity of protein in each tissue sample. (48,49).

I performed all the statistical analysis with the occasional assistance from David Rimm, M.D., Ph.D., Robert Camp, M.D., Ph.D., Annette Molinaro, Ph.D., Jena Giltmore, and Melissa Cregger.

Results

Figure 6 illustrates the final image after RESA, PLACE, and AQUA algorithms are applied to the images captured from the fluorescent stains. The marker in this image, E-cadherin, demonstrates the mostly membranous staining of cadherins. Unfortunately our image resolution does not allow for the distinction between membranous and cytoplasmic staining.

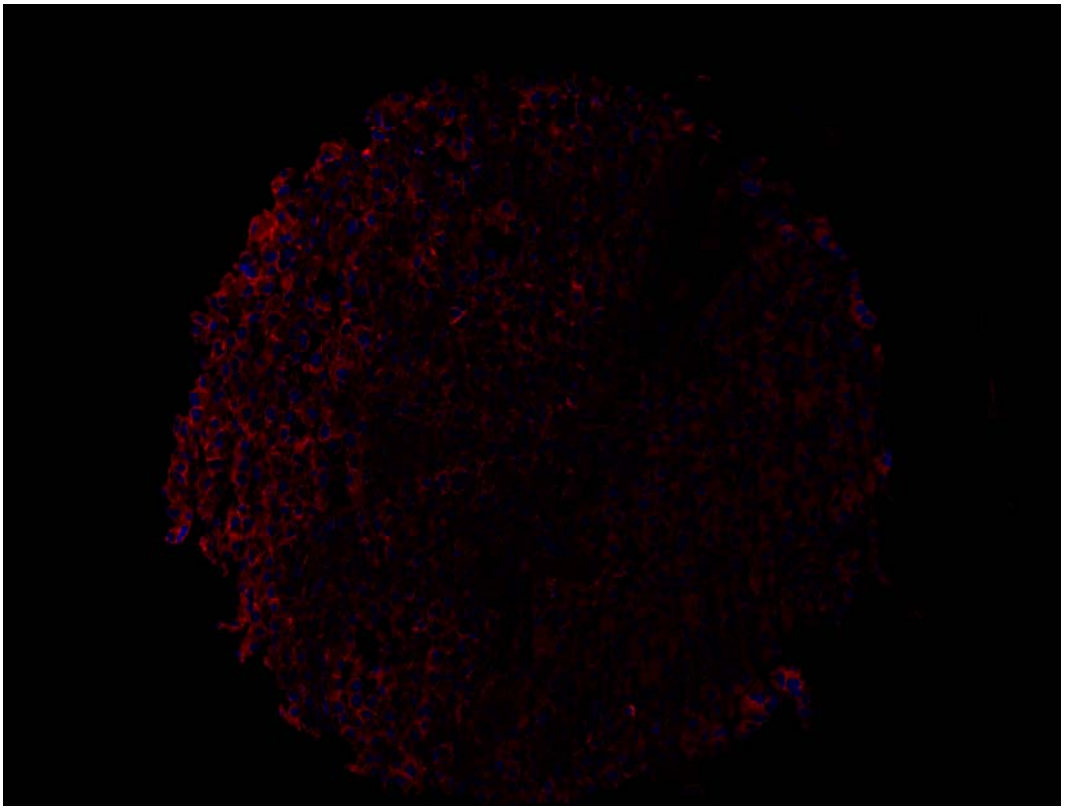

Figure 7. E-Cadherin immunofluorescence after AQUA algorithms of a single histospot.

Figure 7 demonstrates the image captured from S-100 staining, used to identify the area of tumor. Notice normal stroma that is not stained surrounding melanoma tissue. The photo is captured later translated into a binary image, not shown here.

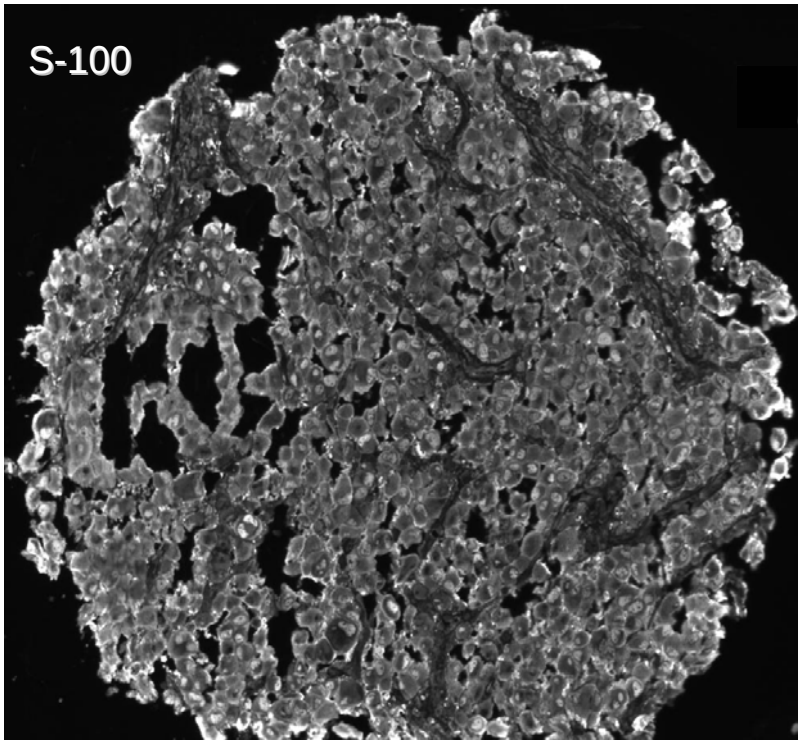

Figure 7. S-100 immunofluorescence of a single histospot.

Figure 8 shows the range and distribution of AQUA scores for alpha-catenin, beta-catenin, p120-catenin, N-cadherin, E-cadherin and P-cadherin. N-cadherin expression clearly was not expressed in a normal distribution; therefore, raw values were normalized prior to analysis with parametric tests.

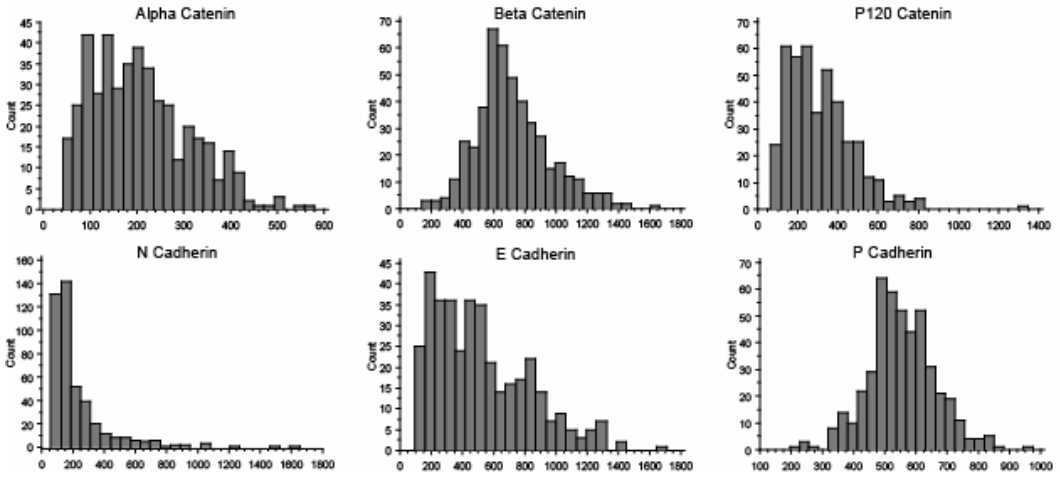

Figure 8. AQUA scores showing range and distribution for alpha-catenin, beta-catenin, p120-catenin, N-cadherin, E cadherin and P-cadherin.

Table 4 shows the average AQUA values for each sub-group of histospots for all analyzed markers.

Table 4. Average tumor mask staining of nevi, primary melanoma, local recurrence melanoma, metastatic melanoma, and melanoma cell lines from YTMA59.

	Alpha-catenin	Beta-catenin	P120-catenin	E-cadherin	N-cadherin	P-cadherin
Nevi	156.512	901.949	358.414	534.688	248.896	641.745
Primary Melanoma	191.239	760.894	286.61	583.53	274.754	566.732
Local Recurrence	222.057	617.096	311.029	625.671	214.202	554.722
Metastatic Melanoma	218.386	703.36	322.897	488.782	197.335	544.113
Melanoma Cell Lines	320.399	1176.666	627.625	888.974	383.261	695.402
ANOVA p-value	<0.0001	<0.0001	<0.0001	0.0004	0.0003	<0.0001

Unpaired T-Tests

We found that mean alpha-catenin expression was the lowest in nevi (156.512) and the highest in melanoma cell lines (320.399). Expression was increased in the primary melanoma patient population (191.239) and significantly increased in the metastatic group (218.386) when compared to regular nevi ($p=0.0131$). The local recurrence population's mean (222.057) was most similar to the metastatic's mean. The averages of primary and metastatic melanomas were significantly different ($p=0.0055$) (Tables 4 and 5).

Beta-catenin also had the highest average expression in melanoma cell lines (1176.66), but the tissue with the lowest expression was local recurrence melanoma (617.096) followed by metastatic melanoma (703.36) and then primary melanoma (760.894). The average nevi and primary tissues had a significant mean difference of

141.046 (p=0.031). Primary and metastatic tissues also were significantly different for beta-catenin (0.0128). Nevi and metastatic melanoma average scores were significantly dissimilar with the largest difference seen in all the scores of 198.59 (p=0.0005).

P120-catenin expression was absolutely the highest in metastatic melanoma tissue (627.625). Primary melanoma tissue showed the lowest average values with a mean of 286.61. Nevi showed average expression of p120-catenin that was much lower than metastatic tissue, however higher than all other specimens (358.414). The only interesting comparison of average values that was significant was the difference between primary and metastatic tissue (p=0.0313).

E-cadherin followed the pattern of extremely high average expression within melanoma cell lines (888.974). Metastatic tissue actually had the lowest mean expression of 488.782. Only the difference between primary and metastatic tissue was significant for E-cadherin (94.748, p=0.0055).

N-cadherin also had the highest mean expression within melanoma cell lines (383.261). Metastatic melanoma was the lowest average expresser (197.335). The difference between primary and metastatic tissue averages was significant (77.419, $p<0.0001$).

Finally, P-cadherin likewise had the highest average AQUA score expressed in melanoma cell lines (695.402). Metastatic melanoma expresses the lowest average score of 544.113. A trend of decreasing average scores was seen from nevi to primary melanoma, to local recurrence, to metastatic melanoma. All comparisons of nevi to primary tissue, primary to metastatic, and nevi to metastatic were significant (75.013,

p=0.0145; 22.619, p=0.0311; and 97.632, p=0.0003, respectively). This trend was only seen with P-cadherin.

Table 5. Unpaired t-tests of all markers.

Alpha-catenin	**Mean Difference**	**T value**	**P Value**
Nevi: Primary	-41.333	-1.407	0.1053
Primary: Metastatic	-29.267	-2.656	0.0055
Nevi: Metastatic	-70.6	-2.237	0.0131
Beta-catenin	**Mean Difference**	**T value**	**P Value**
Nevi: Primary	141.056	2.173	0.031
Primary: Metastatic	57.534	2.499	0.0128
Nevi: Metastatic	198.59	3.51	0.0005
P120-catenin	**Mean Difference**	**T value**	**P Value**
Nevi: Primary	71.804	1.71	0.0891
Primary: Metastatic	-36.287	-2.161	0.0313
Nevi: Metastatic	35.517	0.804	0.422
E-cadherin	**Mean Difference**	**T value**	**P Value**
Nevi: Primary	-48.842	-0.528	0.5985
Primary: Metastatic	94.748	2.794	0.0055
Nevi: Metastatic	45.905	0.509	0.6111
N-cadherin	**Mean Difference**	**T value**	**P Value**
Nevi: Primary	-25.858	-0.524	0.6011
Primary: Metastatic	77.419	3.978	<0.0001

Nevi: Metastatic	51.562	1.131	0.2588

P-cadherin	**Mean Difference**	**T value**	**P Value**
Nevi: Primary	75.013	2.466	0.0145
Primary: Metastatic	22.619	2.163	0.0311
Nevi: Metastatic	97.632	3.689	0.0003

Non-Parametric Spearman Rho Scatterplot Matrix

Correlations of raw AQUA scores among all six protein markers are shown in Figure 9. P-cadherin and beta-catenin express the highest rho value ($r=0.5238$, $p<0.0001$). Beta-catenin shares a similarly strong correlation with E-cadherin ($r=0.4494$, $p<0.0001$). E-cadherin correlates positively with alpha-catenin ($r=0.3592$, $p<0.0001$). P120-catenin shares positive correlations with both alpha and beta-catenins ($r=0.3480$, $p<0.0001$ and $r=0.3638$, $p<0.0001$, respectively).

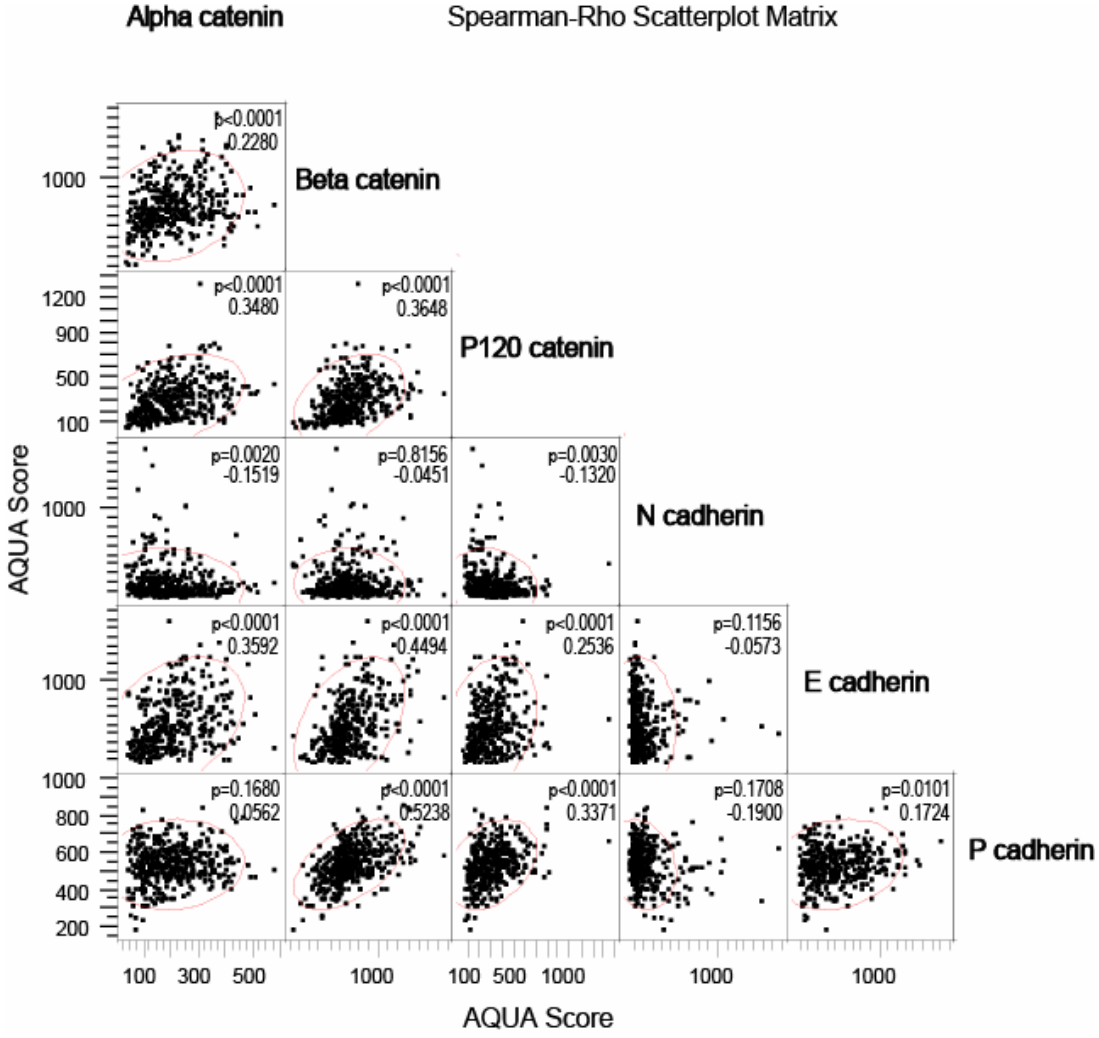

Figure 9. Non-parametric Spearman rho scatterplot matrix depicting similarity in staining intensity of measured cadherins and catenins. P-cadherin and beta-catenin correlate with a rho of 0.5238 ($p<0.0001$). E-cadherin and beta-catenin increase at proportional rates (rho=0.4494, $p<0.0001$). E-cadherin likewise corresponds with alpha-catenin (rho=0.3592, $p<0.0001$). All associations are significant except N-cadherin when paired with E-cadherin, P-cadherin and beta-catenin and the pairing of P-cadherin and alpha-catenin.

However, N-cadherin shows an inverse correlation with all analyzed markers. Besides being reciprocally related, the mesenchymal cadherin shows some of the weakest correlations with other proteins. Although not significant, the correlations with beta-catenin and E-cadherin are the lowest ($r= -0.0451$, $p=0.8156$ and $r= -0.0573$, $p=0.1156$, respectively).

After separating low- and high-expressing melanoma tissue using cut-points created from analysis of our training cohort (50% of original cohort) with X-Tile, raw AQUA scores of non-nuclear N- and E-cadherin significantly predicted patient survival (Figure 10) (p=0.0222 and p=0.0233, respectively). The low expressing N-cadherin (non-nuclear) group had a RR=1.883 (95% CI of 1.099-3.226, p=0.0212). The RR of E-cadherin (non-nuclear) for the low expression group was 1.532 (95% CI of 1.057-2.221, p=0.0243). Univariate analyses of other markers are summarized in Table 5. E- and N-cadherin (non-nuclear) expression did not retain significance when analyzed with Breslow, age, and gender.

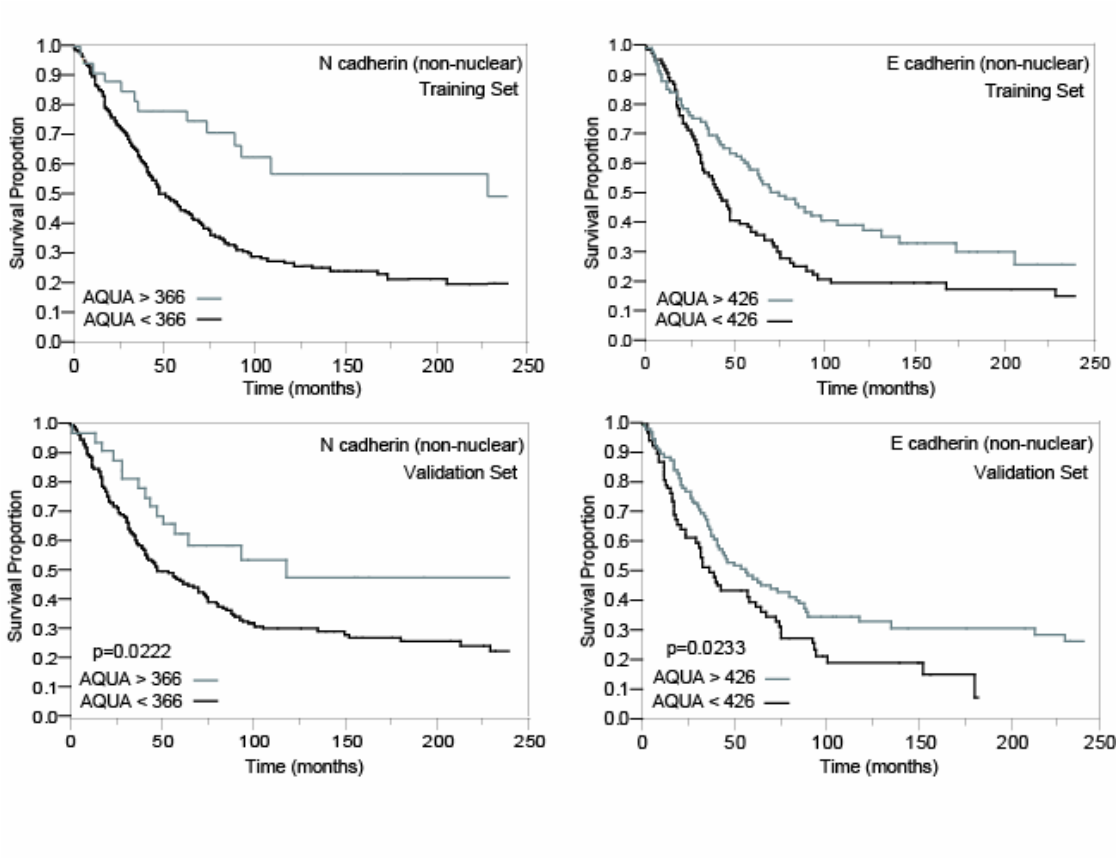

Figure 10. Kaplan-Meier survival curves using cut-points created with X-tile for non-nuclear expression of E-cadherin and N-cadherin. The validation cohort was significant for N-cadherin (non-nuclear) when separating high and low expressing melanomas at an AQUA score of 366 (p=0.0222). The E-cadherin (non nuclear) validation set was significant between high and low expression groups using the X-tile produced cut-point of 426 (p=0.0233).

Table 5. Cox Proportional Hazards univariate and multivariate analysis of markers using X-tile produced cut-points.

Univariate Analysis				
Variable (Low expression)	N	Relative Risk	95% Confidence Interval	P Value
N-cadherin, non-nuclear	201	1.883	1.099-3.226	0.0212
E-cadherin, non-nuclear	164	1.532	1.057-2.221	0.0243
P-cadherin, non-nuclear	207	1.168	0.784-1.740	0.4447
Alpha-catenin	208	0.904	0.644-1.268	0.5578
Beta-catenin	210	1.386	0.908-2.114	0.1300
P120-catenin	186	1.224	0.860-1.740	0.2615
Multivariate Analysis	N	Relative Risk	95% Confidence Interval	P Value
Breslow depth (mm)	94	1.094	0.999-1.198	0.0529
Age at diagnosis (yrs)		1.006	0.985-1.027	0.5886
Gender (female)		0.658	0.351-1.235	0.1928
N-cadherin, non-nuclear (low)		1.77	0.835-3.754	0.1365
Multivariate Analysis	N	Relative Risk	95% Confidence Interval	P Value
Breslow depth (mm)	69	1.109	1.012-1.215	0.0272
Age at diagnosis (yrs)		1.018	0.744-2.616	0.1429
Gender (female)		0.775	0.399-1.504	0.4505
E-cadherin, non-nuclear (low)		1.489	0.785-2.824	0.2223

Hierarchical Clustering

Hierarchical clustering organized melanoma patients into four distinctive clusters that individually shared similar expression profiles (Figure 11A). Only patients who had sufficient protein expression with tumor covering greater than 5% area of the histospot in at least five of six protein markers were included in average-linked clustering. Four clusters were arbitrarily chosen at an equidistant point. Cluster 1 includes 167 patients

who have high expression of alpha-catenin and E-cadherin, but relatively low expression of N-cadherin. These patients had the second highest survival rate of ~25% at 20 years (Figure 11B). Cluster 2 has the lowest survival at 5 years (~27%) and the second lowest at 20 years (~22%). The group includes 31 patients with generally low expression of alpha-catenin and E-cadherin. Cluster 3 has relatively low or average expression of all three cadherins and all three catenins. The survival of these 127 patients is the lowest of the four clusters at 20 years (~12%). Cluster 4 expresses the highest relative levels of N-cadherin compared to other clusters. The 36 patients in cluster 4 had the highest survival at 5 years (~68%) and 20 years (~50%). The survival curves were significant with $p=0.0003$.

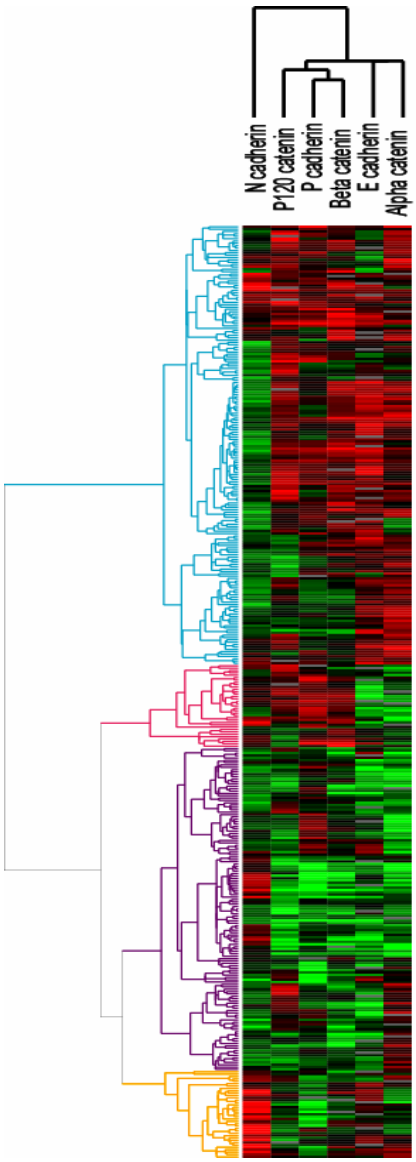

Figure 11A. Hierarchical cluster and survival curve of melanoma patients based on expression of indicated cadherins and catenins.
A. The hierarchical cluster produced by TreeView 1.60 and Cluster 2.11.0.0 (Eisen Software, Berkeley, CA) includes 361 patients who had sufficient protein expression with tumor covering greater than 5% area of the histospot in at least five of six protein markers. Four clusters were arbitrarily chosen at an equidistant point. Red denotes high expression, black is average, and green shows low expression. Cluster 1 (blue) shows 167 patients characterized by high expression of alpha-catenin and E-cadherin with relatively low expression of N-cadherin. Cluster 2 (red) is composed of 31 patients who had melanomas with generally low expression of alpha-catenin and E-cadherin. Cluster 3 (purple) is described by relatively low or average expression of all three cadherins and all three catenins in a total of 127 patients. Cluster 4 (orange) has the highest relative levels of N-cadherin compared to the other patients in the cohort. Other protein expression is varied but generally decreased in the group of 36 patients.

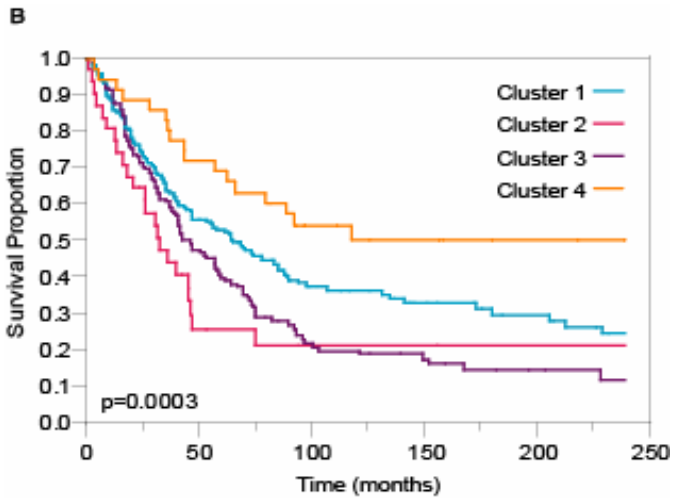

Figure 11B. Kaplan-Meier analysis of the four clusters with 20-year follow-up shows significantly different survival rates (p=0.0003). Cluster 1 had a mean survival of 103.5 months, cluster 2 averaged 37.8 months, cluster 3 averaged 75.0 months, and cluster 4 had a mean of 85.1 months.

The adhesion protein dendrogram created from clustering is perhaps our most interesting result. In accordance with the Kaplan-Meier survival curve and Spearman rho scatterplot matrix, N-cadherin is the most dissimilar to other markers. P-cadherin and beta-catenin share the most similarity.

Discussion

Patterns of Expression

The average expression of all three cadherins was the lowest in metastatic tissue. The next lowest group of tissue was from local recurrence for N- and P-cadherin. Local recurrence tissue is viewed by some as more similar to a metastasis than a primary tumor because of its association with a higher death rate, and this molecular data may support that classification (15).

Cell lines of melanoma showed the overwhelmingly highest averages of expression for all markers (Table 4). Unfortunately, there was no corresponding pattern

of expression in a particular type of *in situ* tissue. As useful as cell lines can be in other studies, our results may reflect the fact that cell lines of melanoma tissue have acquired many mutations that deregulate normal cellular processes. These cells lines may have lost a large number of traits that give them similarity to unmanipulated melanoma tissue.

In Table 5, t-tests show that primary tissue mean expression is statistically different from metastatic melanoma tissue for every marker. This data further suggests that adherens junctional protein regulation is altered as a tumor progresses from a melanoma in situ to a more aggressive type, such as one that would cause metastatic disease.

Biological Interactions of Cadherins and Catenins

Our results summarize previously know biological interactions among cadherins and catenins. We have shown that P-cadherin and beta-catenin have extremely similar expression profiles through Spearman rho correlations and a dendrogram after hierarchical clustering. According to our data p120-catenin and alpha-catenin also share similarity to the former proteins (Figure 11A). The high, positive rho values further strengthen the argument, although alpha-catenin and P-cadherin are not significant in the scatterplot matrix. Our findings reinforce the known binding of alpha-catenin to beta-catenin because of their similar expression profiles and significant positive rho of 0.2280 (Figure 9). Likewise, alpha-catenin is linked to E-cadherin via a connecting protein, beta-catenin (alpha-catenin to E-cadherin rho=0.3592, $p<0.0001$, and beta-catenin to E-cadherin rho=0.4494, $p<0.0001$) (50,51). When downregulation of any one linked

cadherin(s) or catenin(s) occurs, it is logical that other proteins in the complex would follow suit.

Average-linked clustering produced a cluster tree highlighting the biological interactions among the analyzed cadherins and catenins. N-cadherin separates early from the other markers, suggesting that its expression is independent of the other proteins. The two markers that are most closely linked to N-cadherin are E-cadherin and alpha-catenin. Many researchers have highlighted the interaction between E and N-cadherin in melanoma (29,52). Kuphal and Bosserhoff show that the loss of E-cadherin stimulates the up-regulation of N-cadherin via induction of NFκB.

Survival Analysis

We found that moderately high (or maintained) expression of N-cadherin and E-cadherin correlated with improved survival significantly. Our survival curves showing low expression of E-cadherin in non-nuclear compartments confirms previous findings that low E-cadherin is a marker of poor prognosis (27). High expression of alpha-catenin, p120-catenin, and P-cadherin was associated with better survival, although not significant (Table 5). This discovery was contrary to some findings described in the literature, but these studies were mostly qualitative and often did not relate findings to prognosis (29,33,34). We believe that if we could distinguish membranous staining from cytoplasmic staining, we would see alpha-catenin expression only within the cytoplasm – and not the membrane – in these metastatic cells. The potential decrease of catenin at the adherens junction explains the increased mobility of metastatic cells.

Furthermore, Kaplan-Meier curves from hierarchical cluster-generated subpopulations of patients confirmed our hypothesis that patients with overall decreased expression of adherens junctional proteins have decreased survival, possibly due to the cancer's ability to detach from its environment. This subtype of melanoma is consistent with less differentiation and increased motility ability. Cluster 3, the subgroup with generally low expression of all tested adhesion proteins, has the absolute lowest survival rate from our cohort (Figure 11B).

The overall decrease in N-cadherin and beta-catenin expression in metastatic melanoma suggests that adherens junctions deteriorate in cells that become metastatic. Our findings support one of the requirements for metastatic melanoma; malignant cells must be able to disassociate from neighboring cells to become metastatic.

We found that some of the select cadherins and catenins were up- and down-regulated in a fashion that was not found to be independently significant. However, when the six markers were analyzed in an algorithm that made use of all quantitated data, we found that patients could be organized into distinct subgroups. These groups differed by the amount and type of adhesion-complex protein expressed. When these groups were plotted on a Kaplan-Meier curve, the prognosis of one population was significantly different than other populations.

Just as the five proteins described above are similar in expression and allow us to group patients into clusters with poor survival, strong expression of N-cadherin defines a subpopulation of patients with the best survival of our cohort. Our findings are contrary to previously reported epithelial-to-mesenchymal transition (EMT) studies. The EMT describes the change in expression of adhesion proteins when a malignancy transforms

into a more aggressive tumor. Some literature suggests that malignant conversion occurs via NFκB signaling in melanoma. Downregulation of E-cadherin stimulates N-cadherin, which is described as "cadherin switching" (53). However, the increase in N-cadherin is shown in cell lines and has not been analyzed in regard to prognosis. Our data summarizes a subpopulation of melanoma patients, and the EMT melanomas may be describing a different class. Additionally, neural crest derived melanomas may be entirely different from the epithelial carcinomas that have previously shown cadherin switching. Cadherin switching may indicate more aggressive disease in epithelial derived tumors, but in melanomas that are derived from the neural crest, retaining N-cadherin may indicated a more highly differentiated tumor since the expression resembles a mature melanocyte.

Limitations to our work include the problems encountered when dividing a cohort into training and validation sets. Because we used a separate set of patients to determine cut points for the validation set, we did not train the X-Tile tests on the same cohort of patients. This should ensure the quality of our findings, however limiting the final number of patients that could be included in analysis. Other limitations include the inability to directly measure cytoplasmic, or even more specifically membranous, expression of cadherins. While a more precise "membranous mask" would give our experiments further accuracy, the catenin proteins were properly measured in the entirety of the tumor. Catenins can be found in the cytoplasm and nucleus, as well as attached to E-cadherin complexes or individually placed within the cell (50). Although we attempted to include gamma-catenin in our studies, heterogeneous staining presumably due to a nonspecific antibody prevented us from presenting a more complete picture of the

adhesion proteins in melanoma. Alternatively, gamma-catenin may be expressed at very low levels in melanoma, and our staining methods did not allow for accurate assessment.

In summary, the expression profile of tumors reflects known biological interactions of cadherins and catenins. Our scatterplot matrix and biomarker dendrogram exemplified the relationships. Molecular classification using AQUA technology may identify less aggressive sub-types of melanoma.

We identified at least two subclasses of melanoma that correlate with survival: 1) one with strong expression of N-cadherin, which identifies patients with the best survival of our cohort; and 2) a second subclass with a very poor outcome that includes two distinctive molecular classes: A) one with downregulation of essentially all the cadherin-catenin complex proteins as would be seen in a poorly differentiated tumor; and B) another that includes patients with high levels of all the cadherin-catenin proteins consistent with an epithelioid type of melanoma.

More recent work in our laboratory has shown that after stratifying the cohort into primary and metastatic disease, our results hold true when analyzing simply primary tissue. These results would allow for even earlier identification of aggressive subtypes of melanoma, therefore, possibly alleviating the need of a SLNB. Clinicians would be able to recognize patients with more aggressive forms of melanoma even before metastasis occurs, allowing quicker and possibly more targeted forms of therapy. Immediate practical application of this work includes the ability to classify patients into clearer and more precise sub-groups based on the aggressiveness of disease. This will allow clinicians to determine which patients may benefit from certain therapeutics, when successful adjuvant therapies are identified.

Our findings are consistent with Bittner, Onken, and Alonso (10,11,14). Our study expands on their work by showing that molecular classification of melanoma correlates with survival and can indicate prognosis. Our bench-work science clearly can be applied to the bedside, and may benefit melanoma patients in the near future.

Future studies in this area could use larger cohorts of purely primary tissue to further strengthen the power of the analysis. Once a validated antibody of gamma-catenin can effectively stain melanoma tissue, more complete analysis of the cadherin and catenin family can occur. Other markers such as phosphorylated beta-catenin and cadherin 11 can be explored as well. We had difficulty obtaining precise and accurate staining with these antibodies. Additionally, further refinements in technique will allow for quantification of biomarkers within more precise areas of the cell, such as purely cytoplasmic, membranous, or nuclear-membranous staining. Further statistical exploration with a larger cohort might produce a predictor model that can be used in clinical practice. Later studies could use aggressive-disease melanoma tissue identified through the predictor model to test the efficacy of treatment modalities. Adjuvant therapy is only used in late stages of melanoma, but early treatment to this subgroup of patients might prove to be more effective. Furthermore, treating specific subgroups of melanoma patients might reveal a higher response rate and greater effect on survival if we are able to identify subtype-specific treatments, like the advancements seen in estrogen receptor positive breast malignancies.

References

(1) Ries LAG, Eisner MP, Kosary CL, Hankey BF, Miller BA, Clegg L, et al. *SEER Cancer Statistics Review, 1975-2002*, National Cancer Institute. Bethesda, MD. 2004; Available at: http://seer.cancer.gov/csr/1975_2002/. Accessed 12/21, 2005.

(2) American Cancer Society. Facts and Figures. 2006.

(3) Balch CM, Buzaid AC, Soong SJ, Atkins MB, Cascinelli N, Coit DG, et al. Final version of the American Joint Committee on Cancer staging system for cutaneous melanoma. J.Clin.Oncol. 2001 Aug 15;19(16):3635-3648.

(4) Kim K, Pang KM, Evans M, Hay ED. Overexpression of beta-catenin induces apoptosis independent of its transactivation function with LEF-1 or the involvement of major G1 cell cycle regulators. Mol.Biol.Cell 2000 Oct;11(10):3509-3523.

(5) Messina JL, Glass LF, Cruse CW, Berman C, Ku NK, Reintgen DS. Pathologic examination of the sentinel lymph node in malignant melanoma. Am.J.Surg.Pathol. 1999 Jun;23(6):686-690.

(6) Morton DL, Thompson JF, Cochran AJ, Mozzillo N, Elashoff R, Essner R, et al. Sentinel-node biopsy or nodal observation in melanoma. N.Engl.J.Med. 2006 Sep 28;355(13):1307-1317.

(7) Ribuffo D, Gradilone A, Vonella M, Chiummariello S, Cigna E, Haliassos N, et al. Prognostic significance of reverse transcriptase-polymerase chain reaction-negative sentinel nodes in malignant melanoma. Ann.Surg.Oncol. 2003 May;10(4):396-402.

(8) Ranieri JM, Wagner JD, Wenck S, Johnson CS, Coleman JJ,3rd. The prognostic importance of sentinel lymph node biopsy in thin melanoma. Ann.Surg.Oncol. 2006 Jul;13(7):927-932.

(9) Kim CJ, Reintgen DS, Balch CM, AJCC Melanoma Staging Committee. The new melanoma staging system. Cancer Control 2002 Jan-Feb;9(1):9-15.

(10) Bittner M, Meltzer P, Chen Y, Jiang Y, Seftor E, Hendrix M, et al. Molecular classification of cutaneous malignant melanoma by gene expression profiling. Nature 2000 Aug 3;406(6795):536-540.

(11) Onken MD, Ehlers JP, Worley LA, Makita J, Yokota Y, Harbour JW. Functional gene expression analysis uncovers phenotypic switch in aggressive uveal melanomas. Cancer Res. 2006 May 1;66(9):4602-4609.

(12) Hoek K, Rimm DL, Williams KR, Zhao H, Ariyan S, Lin A, et al. Expression profiling reveals novel pathways in the transformation of melanocytes to melanomas. Cancer Res. 2004 Aug 1;64(15):5270-5282.

(13) Bastian BC, Kashani-Sabet M, Hamm H, Godfrey T, Moore DH,2nd, Brocker EB, et al. Gene amplifications characterize acral melanoma and permit the detection of occult tumor cells in the surrounding skin. Cancer Res. 2000 Apr 1;60(7):1968-1973.

(14) Alonso SR, Ortiz P, Pollan M, Perez-Gomez B, Sanchez L, Acuna MJ, et al. Progression in cutaneous malignant melanoma is associated with distinct expression profiles: a tissue microarray-based study. Am.J.Pathol. 2004 Jan;164(1):193-203.

(15) Reintgen D. Establishing a standard of care for the patient with melanoma. Ann.Surg.Oncol. 2001 Mar;8(2):91.

(16) Balch CM, Soong SJ, Smith T, Ross MI, Urist MM, Karakousis CP, et al. Long-term results of a prospective surgical trial comparing 2 cm vs. 4 cm excision margins for 740 patients with 1-4 mm melanomas. Ann.Surg.Oncol. 2001 Mar;8(2):101-108.

(17) Otley CC. Sentinel lymph node biopsy for melanoma--standard of care? Dermatol.Surg. 2000 Nov;26(11):1067-1069.

(18) Gogas HJ, Kirkwood JM, Sondak VK. Chemotherapy for metastatic melanoma: time for a change? Cancer 2007 Jan 2.

(19) Eggermont AM, Kirkwood JM. Re-evaluating the role of dacarbazine in metastatic melanoma: what have we learned in 30 years? Eur.J.Cancer 2004 Aug;40(12):1825-1836.

(20) Neri B, Vannozzi L, Fulignati C, Pantaleo P, Pantalone D, Paoletti C, et al. Long-term survival in metastatic melanoma patients treated with sequential biochemotherapy: report of a Phase II study. Cancer Invest. 2006 Aug-Sep;24(5):474-478.

(21) Birchmeier W, Weidner KM, Hulsken J, Behrens J. Molecular mechanisms leading to cell junction (cadherin) deficiency in invasive carcinomas. Semin.Cancer Biol. 1993 Aug;4(4):231-239.

(22) Voura EB, Sandig M, Kalnins VI, Siu C. Cell shape changes and cytoskeleton reorganization during transendothelial migration of human melanoma cells. Cell Tissue Res. 1998 Sep;293(3):375-387.

(23) Huber O, Bierkamp C, Kemler R. Cadherins and catenins in development. Curr.Opin.Cell Biol. 1996 Oct;8(5):685-691.

(24) Takayama T, Shiozaki H, Shibamoto S, Oka H, Kimura Y, Tamura S, et al. Beta-catenin expression in human cancers. Am.J.Pathol. 1996 Jan;148(1):39-46.

(25) Shiozaki H, Iihara K, Oka H, Kadowaki T, Matsui S, Gofuku J, et al. Immunohistochemical detection of alpha-catenin expression in human cancers. Am.J.Pathol. 1994 Apr;144(4):667-674.

(26) Hashizume R, Koizumi H, Ihara A, Ohta T, Uchikoshi T. Expression of beta-catenin in normal breast tissue and breast carcinoma: a comparative study with epithelial cadherin and alpha-catenin. Histopathology 1996 Aug;29(2):139-146.

(27) Andersen K, Nesland JM, Holm R, Florenes VA, Fodstad O, Maelandsmo GM. Expression of S100A4 combined with reduced E-cadherin expression predicts patient outcome in malignant melanoma. Mod.Pathol. 2004 Aug;17(8):990-997.

(28) Seline PC, Norris DA, Horikawa T, Fujita M, Middleton MH, Morelli JG. Expression of E and P-cadherin by melanoma cells decreases in progressive melanomas and following ultraviolet radiation. J.Invest.Dermatol. 1996 Jun;106(6):1320-1324.

(29) Sanders DS, Blessing K, Hassan GA, Bruton R, Marsden JR, Jankowski J. Alterations in cadherin and catenin expression during the biological progression of melanocytic tumours. Mol.Pathol. 1999 Jun;52(3):151-157.

(30) Pacifico MD, Grover R, Richman PI, Buffa F, Daley FM, Wilson GD. Identification of P-cadherin in primary melanoma using a tissue microarrayer: prognostic implications in a patient cohort with long-term follow up. Ann.Plast.Surg. 2005 Sep;55(3):316-320.

(31) Van Marck V, Stove C, Van Den Bossche K, Stove V, Paredes J, Vander Haeghen Y, et al. P-cadherin promotes cell-cell adhesion and counteracts invasion in human melanoma. Cancer Res. 2005 Oct 1;65(19):8774-8783.

(32) Bachmann IM, Straume O, Puntervoll HE, Kalvenes MB, Akslen LA. Importance of P-cadherin, beta-catenin, and Wnt5a/frizzled for progression of melanocytic tumors and prognosis in cutaneous melanoma. Clin.Cancer Res. 2005 Dec 15;11(24 Pt 1):8606-8614.

(33) Zhang XD, Hersey P. Expression of catenins and p120cas in melanocytic nevi and cutaneous melanoma: deficient alpha-catenin expression is associated with melanoma progression. Pathology 1999 Aug;31(3):239-246.

(34) Krengel S, Groteluschen F, Bartsch S, Tronnier M. Cadherin expression pattern in melanocytic tumors more likely depends on the melanocyte environment than on tumor cell progression. J.Cutan.Pathol. 2004 Jan;31(1):1-7.

(35) DeVita VT, Hellman S, Rosenberg SA. Cancer, principles & practice of oncology. Philadelphia, PA: Lippincott Williams & Wilkins; 2005. p. 2898-2898.

(36) DiVito KA, Charette LA, Rimm DL, Camp RL. Long-term preservation of antigenicity on tissue microarrays. Lab.Invest. 2004 Aug;84(8):1071-1078.

(37) Coons AH, Creech HJ, Jones RN. Immunological propterties of an antibody containing a fluorescent group. Proc. Soc. Exp. Biol. Med. 1941;Vol. 47:200--202.

(38) Cattoretti G, Ellis R, Kiernan J, Miller R, Peters S, Richmond R, et al. Immunohistochemistry World: Introduction to Immunohistochemistry. 2005; Available at: http://www.ihcworld.com/introduction.htm#intro. Accessed 1/12, 2007.

(39) Camp RL, Chung GG, Rimm DL. Automated subcellular localization and quantification of protein expression in tissue microarrays. Nat.Med. 2002 Nov;8(11):1323-1327.

(40) Dolled-Filhart M, McCabe A, Giltnane J, Cregger M, Camp RL, Rimm DL. Quantitative in situ analysis of beta-catenin expression in breast cancer shows decreased expression is associated with poor outcome. Cancer Res. 2006 May 15;66(10):5487-5494.

(41) Dillon DA, D'Aquila T, Reynolds AB, Fearon ER, Rimm DL. The expression of p120ctn protein in breast cancer is independent of alpha- and beta-catenin and E-cadherin. Am.J.Pathol. 1998 Jan;152(1):75-82.

(42) Reyes-Mugica M, Meyerhardt JA, Rzasa J, Rimm DL, Johnson KR, Wheelock MJ, et al. Truncated DCC reduces N-cadherin/catenin expression and calcium-dependent cell adhesion in neuroblastoma cells. Lab.Invest. 2001 Feb;81(2):201-210.

(43) Cho KH, Hashimoto K, Taniguchi Y, Pietruk T, Zarbo RJ, An T. Immunohistochemical study of melanocytic nevus and malignant melanoma with monoclonal antibodies against S-100 subunits. Cancer 1990 Aug 15;66(4):765-771.

(44) Gordis L. Epidemiology. 2nd ed. Philadelphia: W.B. Saunders; 2000.

(45) Environmental Systems Research Institute, Inc. Scatterplot. 2002; Available at: http://edndoc.esri.com/arcobjects/8.3/Samples/Analysis%20and%20Visualization/Scatterplot/Scatterplot.htm. Accessed 1/12, 2007.

(46) Lane DM. HyperStat Online Statistics Textbook: Spearman's rho. 2006; Available at: http://davidmlane.com/hyperstat/A62436.html. Accessed 1/12, 2007.

(47) Camp RL, Dolled-Filhart M, Rimm DL. X-tile: a new bio-informatics tool for biomarker assessment and outcome-based cut-point optimization. Clin.Cancer Res. 2004 Nov 1;10(21):7252-7259.

(48) Chipman H, Tibshirani R. Hybrid hierarchical clustering with applications to microarray data. Biostatistics 2006 Apr;7(2):286-301.

(49) Guess MJ, Wilson SB. Introduction to hierarchical clustering. J.Clin.Neurophysiol. 2002 Apr;19(2):144-151.

(50) Hinck L, Nathke IS, Papkoff J, Nelson WJ. Dynamics of cadherin/catenin complex formation: novel protein interactions and pathways of complex assembly. J.Cell Biol. 1994 Jun;125(6):1327-1340.

(51) Rimm DL, Koslov ER, Kebriaei P, Cianci CD, Morrow JS. Alpha 1(E)-catenin is an actin-binding and -bundling protein mediating the attachment of F-actin to the membrane adhesion complex. Proc.Natl.Acad.Sci.U.S.A. 1995 Sep 12;92(19):8813-8817.

(52) Kuphal S, Poser I, Jobin C, Hellerbrand C, Bosserhoff AK. Loss of E-cadherin leads to upregulation of NFkappaB activity in malignant melanoma. Oncogene 2004 Nov 4;23(52):8509-8519.

(53) Kuphal S, Bosserhoff AK. Influence of the cytoplasmic domain of E-cadherin on endogenous N-cadherin expression in malignant melanoma. Oncogene 2006 Jan 12;25(2):248-259.